DOI: 10.1093/jnci/djs140
Advance Access publication on March 27, 2012.

ARTICLE

Therapeutic Potential of Amanitin-Conjugated Anti-Epithelial Cell Adhesion Molecule Monoclonal Antibody Against Pancreatic Carcinoma

Gerhard Moldenhauer, Alexei V. Salnikov, Sandra Lüttgau, Ingrid Herr, Jan Anderl, Heinz Faulstich

Manuscript received June 16, 2011; revised February 1, 2012; accepted February 3, 2012.

Correspondence to: Gerhard Moldenhauer, MD, Department of Translational Immunology (D015), German Cancer Research Center, Im Neuenheimer Feld 280, Heidelberg 69120, Germany (e-mail: g.moldenhauer@dkfz.de).

Background Human epithelial cell adhesion molecule (EpCAM) is overexpressed in many cancers. Anti-EpCAM antibodies have shown promise in preclinical studies, but showed no tumor regression in a recent phase II clinical trial. Therefore, we generated a novel anti-EpCAM antibody–drug conjugate and assessed whether it showed enhanced antitumor effects.

Methods Chemical cross-linking was conducted to covalently conjugate α-amanitin, a toxin known to inhibit DNA transcription, with chiHEA125, a chimerized anti-EpCAM monoclonal antibody, to generate the antibody–drug conjugate α-amanitin-glutarate-chiHEA125 (chiHEA125-Ama). Antiproliferative activity of chiHEA125-Ama was tested in human pancreatic (BxPc-3 and Capan-1), colorectal (Colo205), breast (MCF-7), and bile duct (OZ) cancer cell lines in vitro using [^{3}H]-thymidine incorporation assay. Antitumor activity of chiHEA125-Ama was assessed in vivo in immunocompromised mice bearing subcutaneous human BxPc-3 pancreatic carcinoma xenograft tumors (n = 66 mice). Cell proliferation and apoptosis were evaluated in xenograft tumors by immunohistochemistry. All statistical tests were two-sided.

Results In all cell lines, chiHEA125-Ama reduced cell proliferation (mean half maximal inhibitory concentration [IC_{50}] = 2.5×10^{-10} to 5.4×10^{-12} M). A single dose of chiHEA125-Ama inhibited BxPc-3 xenograft tumor growth (chiHEA125 [control, n = 4 mice] vs chiHEA125-Ama [n = 6 mice], dose of 15 mg/kg with respect to IgG and 50 μg/kg with respect to α-amanitin, mean relative increase in tumor volume on day 16 = 884% vs −79%, difference = 963%, 95% CI = 582% to 1344%, $P = .019$). Two higher doses of chiHEA125-Ama (100 μg/kg with respect to α-amanitin), administered 1 week apart (n = 10 mice per group), led to complete tumor regression in nine of 10 (90%) mice compared with chiHEA125, during the observation period of 16 days; increased apoptosis and reduced cell proliferation were observed in mice treated with chiHEA125-Ama.

Conclusion This preclinical study suggests that anti-EpCAM antibody conjugates with α-amanitin have the potential to be highly effective therapeutic agents for pancreatic carcinomas and various EpCAM-expressing malignancies.

J Natl Cancer Inst 2012;104:622–634

Pancreatic cancer is one of the most aggressive malignancies and the fourth leading cause of cancer deaths in the United States with the lowest 5-year survival rate of approximately 3% (1). Pancreatic cancer patients have limited therapeutic options with curative surgery, which is only possible for a very small number of physically fit patients with local disease (2). Therefore, new treatment modalities for pancreatic cancer are urgently needed.

Cancer immunotherapy with antibodies and immunotoxins has attracted increased attention following the advancement in technologies for the development of therapeutic antibodies. The epithelial cell adhesion molecule (EpCAM), also known as cluster of differentiation 326 (CD326), is one of the best-studied target antigens on human tumors (3,4). It represents a type I membrane glycoprotein of 314 amino acids with an apparent molecular weight of 40 kDa (5). EpCAM is overexpressed in the majority of adenocarcinomas, including pancreatic adenocarcinoma, cholangiocarcinoma, node-positive breast cancer, epithelial ovarian cancer, and squamous cell head and neck cancer (6,7). An increased EpCAM expression is a poor prognostic marker in breast and gallbladder carcinomas (8–11). Importantly, EpCAM is expressed by tumor-initiating cells, also known as cancer stem cells in pancreatic and colorectal adenocarcinomas, and in breast carcinomas (12–14).

Several anti-EpCAM therapeutic antibodies have been developed (edrecolomab, ING-1, 3622W94, adecatumumab) and used in anticancer studies with promising results [reviewed in (15,16)]. The proposed mechanisms of their antitumor effects involve antibody-dependent cellular cytotoxicity and complement-mediated

cytotoxicity (17,18). The most prominent example is adecatumumab (MT201), a fully human anti-EpCAM antibody, which was well tolerated by patients with hormone-refractory prostate cancer (19) and in patients with rising prostate-specific antigen (PSA) levels after the radical prostatectomy (20). Despite initial concerns regarding pancreatic toxicity of anti-EpCAM antibody, the most recent phase II clinical trial in metastatic breast cancer patients has confirmed the overall safety of monotherapy with adecatumumab and showed some therapeutic activity in the clinic; however, no objective tumor regression could be observed (21). Therefore, it seems reasonable to probe the enhancement of the antitumor effects of EpCAM-directed antibody therapy via generation of an antibody–drug conjugate (ADC). This notion is further supported by the findings that ADCs have greater antitumor activity than the antibody alone, as shown in colorectal tumors for SWA11-ZZ-PE38 ADC containing a *Pseudomonas aeruginosa* exotoxin derivative PE38 and directed against CD24 antigen (22), in colon and renal adenocarcinomas for maytansinoid DM1-conjugated anti-EpCAM monoclonal antibody (mAb) B38.1 ADC (23), in mouse xenograft models of anaplastic large cell lymphoma or Hodgkin's disease for monomethyl auristatin E–conjugated anti-CD30 mAb cAC10 (24,25) and for several other ADCs, which are currently in clinical development [reviewed in (26)].

In this study, we developed a novel therapeutic ADC α-amanitin-glutarate-chiHEA125 (chiHEA125-Ama) by conjugating a mushroom toxin, α-amanitin, to an EpCAM-specific chimerized mAb chiHEA125 developed in our laboratory. α-amanitin is the main component of the amatoxins, which are cyclic octapeptides produced by basidiomycetes mushrooms, particularly of the genus *Amanita*, but also by some species of the genus *Galerina* and *Lepiota* [reviewed in (27–29)]. Amatoxins are the products of a ribosomal synthesis followed by posttranslational modifications such as cyclization and hydroxylation of the side chains of the eight amino acids (30) and bind to RNA-polymerase II of eukaryotic cells with the highest affinity (dissociation constant [K_D] of approximately 10^{-9} M) found for mammalian enzymes (31,32). In mammalian cells, inhibition of DNA transcription by amatoxins leads to apoptosis (33). We investigated antitumor activity of the chiHEA125-Ama against multiple cancer cell lines in vitro. The therapeutic potential of the chiHEA125-Ama was assessed in a human pancreatic carcinoma mouse xenograft model, and treatment-related toxicity was evaluated in mice.

CONTEXTS AND CAVEATS

Prior knowledge

The epithelial cell adhesion molecule (EpCAM) is expressed in many human tumors. Despite the promising antitumor activities of anti-EpCAM antibodies, no breast tumor regression was observed in a recent phase II trial.

Study design

A novel anti-EpCAM antibody-α-amanitin drug conjugate (chiHEA125-Ama) was generated to assess enhanced antitumor activity compared with the unconjugated antibody (chiHEA125). Antiproliferative activity was tested in vitro using human cancer cell lines, and antitumor activity was evaluated in vivo using a mouse xenograft model bearing subcutaneous human pancreatic tumors.

Contribution

ChiHEA125-Ama showed a strong antiproliferative activity in vitro and a strong inhibition of xenograft pancreatic tumor growth in vivo.

Implication

This antibody–drug conjugate has the potential to be an effective therapeutic agent for pancreatic cancer and various EpCAM-expressing malignancies.

Limitations

Dose-limiting toxicity in human patients cannot be ruled out. Results of this preclinical study conducted in mice may not be translatable to humans.

From the Editors

Materials and Methods

Cell Lines and Reagents

Human pancreatic cell lines BxPc-3 and Capan-1, human colorectal cell line Colo205, human breast cancer cell line MCF-7, and human bile duct cancer cell line OZ were obtained from the American Type Culture Collection (Manassas, VA). The cell lines were authenticated by the German Resource Centre for Biological Material (Braunschweig, Germany) and throughout the culture by assessment of typical morphology by the investigators. Mycoplasma-negative cultures were ensured by weekly tests. Cells were cultured in RPMI-1640 medium (Sigma-Aldrich, Deisenhofen, Germany) supplemented with 10% heat-inactivated fetal calf serum (FCS) (Biochrom, Berlin, Germany), 2 mM L-glutamine (Invitrogen, Karlsruhe, Germany), and 1 mM sodium pyruvate (Invitrogen) (complete medium). All cells were maintained in a humidified atmosphere at 37°C and 5% CO_2.

Synthesis of Chimeric Antibody chiHEA125

Several years ago, our group established a hybridoma cell line secreting the anti-EpCAM mouse mAb HEA125 (34,35). Using homologous recombination technique, this hybridoma line was reconstructed to produce a mouse–human chimerized version of the antibody consisting of the mouse variable domains joined with human kappa constant light chain and human IgG_1 constant heavy chain. The resulting antibody chiHEA125 binds to EpCAM-expressing cells with high affinity (K_D of approximately 2.2×10^{-9} M) and high specificity (S. Lüttgau , U. Kutay, A. Poustka, G. Moldenhauer, F. Breitling, unpublished data, and Supplementary Figure 1, available online). ChiHEA125 was purified by affinity chromatography using a protein A-Sepharose CL-4B column (GE Healthcare, München, Germany). Antibody concentration was measured with a NanoDrop ND-2000c spectrophotometer (Peqlab Biotechnologie, Erlangen, Germany). The control antibody omalizumab (trade name Xolair), which is a human IgG_1 antibody directed against human IgE immunoglobulin, was purchased from Novartis (Basel, Switzerland).

Synthesis of chiHEA125-Ama and α-Amanitin-Glutarate-Omalizumab (Omalizumab-Ama)

α-amanitin was attached to immunoglobulin molecules by the glutarate linkage intended to release free α-amanitin inside the

tumor cell when in contact with esterases or proteases. Modification of the dihydroxylated isoleucin of α-amanitin with glutaric anhydride retains α-amanitin RNA-polymerase II inhibitory activity (data not shown). α-amanitin (3.0 mg [3.3 μmol]) (Sigma-Aldrich), dried in vacuo over P_4O_{10}, was dissolved in 0.25 mL of dry pyridine (Sigma-Aldrich) and was allowed to react with 0.9 mg (79 μmol) glutaric anhydride (Sigma-Aldrich) in 0.1 mL pyridine at room temperature in the dark for 24 hours. The peptide was precipitated by addition of 7 mL of dry diethylether (Sigma-Aldrich) and centrifuged at 2000*g* at 4°C for 15 minutes using Heraeus Instruments Megafuge 1.0R (Thermo Fisher Scientific, Waltham, MA). The solid precipitate was washed a second time with diethylether and centrifuged as mentioned above. α-amanitin-glutarate (3.4 mg [3.3 μmol]) was dissolved in 0.05 mL of dry dimethylformamide (DMF) (Sigma-Aldrich) and 2.4 mg (seven equivalents of α-amanitin glutarate) of N-hydroxysuccinimide (Sigma-Aldrich) dissolved in 0.01 mL of DMF was added to it. After addition of 1.2 mg of dicyclohexylcarbodiimide (Sigma-Aldrich) in 0.01 mL of DMF, the reaction was allowed to proceed for 16 hours at room temperature. The solution was separated from the formed crystals, and the peptide was precipitated by adding 4 mL of dry diethylether. After centrifugation at 2000*g* at 4°C for 15 minutes, the pellet was washed with 4 mL of diethylether and centrifuged again. The solid precipitate was dissolved in 0.1 mL of DMF and added to 10 mg of chiHEA125 or omalizumab mAb in 5 mL of phosphate-buffered saline (PBS) and was allowed to react under slow rotation at 5°C in the dark. After 16 hours, the solution was applied to a Sephadex G25 column (120 × 1.5 cm) (GE Healthcare) equilibrated with Dulbecco's PBS pH 7.4 (Invitrogen), and the protein fraction was collected. α-amanitin:IgG ratio in the newly synthesized ADC chiHEA125-Ama or omalizumab-Ama was determined spectrophotometrically (Specord 210 Plus; Analytik Jena, Jena, Germany) from the absorption difference at 310 nm of the protein solution against a blank control containing the same concentration of the nonconjugated antibody using the molar extinction coefficient for amatoxins of 13 500 M^{-1} cm^{-1} and calculation according to the Beer–Lambert law. The ratio α-amanitin:IgG molecule varied from 4:1 to 8:1. Biochemical characteristics of chiHEA125-Ama were evaluated by high performance liquid chromatography (HPLC) using a PlatinBlue HPLC system (Knauer, Berlin, Germany) with a TSKgel SuperSW3000 size-exclusion chromatography column (30 cm × 4.6 mm) (Tosoh Bioscience, Tokyo, Japan) and a running buffer (0.2 M potassium phosphate, 0.2 M potassium chloride, 15% 2-propanol, pH 6.8) at 0.35 mL/min. In addition, chiHEA125 and chiHEA125-Ama were analyzed by reducing sodium dodecyl sulfate–polyacrylamide gel electrophoresis (SDS-PAGE) and Coomassie staining according to common procedures. Immunoblot analysis of 30 ng chiHEA125 and chiHEA125-Ama was done by standard techniques. α-amanitin was detected with an antiserum obtained by immunization of rabbits with a fetuin-β-amanitin conjugate (36).

Binding Competition Assay and Flow Cytometry

Binding of ADC chiHEA125-Ama vs nonconjugated chiHEA125 antibody to Colo205 cells was analyzed in a binding competition assay by flow cytometry. Colo205 cells were washed twice in fluorescence-activated cell sorting (FACS) buffer (Dulbecco's PBS pH 7.4 [Invitrogen] with 1% heat-inactivated FCS [Biochrom] and 0.1% sodium azide [Merck, Darmstadt, Germany]), and 50 μL of cell suspension (2×10^7 cells per mL) was added to each well of a 96-well U-bottom microtiter plate (Techno Plastic Products, Trasadingen, Switzerland), and fluorescein (FITC)-labeled chiHEA125 antibody (50 μL per well) was added. Serial dilutions of chiHEA125-Ama or chiHEA125 ranging from 400 μg/mL to 10 ng/mL of IgG at final dilution (corresponding to a range of 2.7×10^{-6} to 6.7×10^{-11} M IgG, and with respect to α-amanitin content in chiHEA125-Ama, it ranged from 1.1×10^{-5} M [10.1 μg/mL] to 2.4×10^{-12} M [1.8 pg/mL]) were added in triplicates in a volume of 50 μL per well and incubated for 1 hour on ice. Subsequently, the plate was centrifuged at 600*g* at 4°C using a Minifuge GL centrifuge (Heraeus-Christ, Osterode, Germany) for 2 minutes, and the supernatant was removed from the wells. The cells were resuspended in 150 μL of FACS buffer and centrifuged again as above. After washing twice with the FACS buffer, the cells were added to 100 μL per well of propidium iodide solution (Merck) (1 μg/mL in FACS buffer) allowing discrimination of dead cells. The analysis was performed on a FACScan cytometer (Becton and Dickinson, Heidelberg, Germany), and mean fluorescence intensity was quantified using CellQuest software. Two independent experiments in triplicates were performed.

Flow Cytometry Analysis of EpCAM Expression in Cancer Cell Lines

EpCAM expression of various tumor cell lines was determined by indirect flow cytometry. For this, BxPc-3, Capan-1, Colo205, MCF-7, and OZ cells (1×10^6) were first incubated for 1 hour with 100 μL of chiHEA125 mAb diluted 1:50 in the FACS buffer kept on ice followed by 1 hour incubation with FITC-labeled $F(ab')_2$ goat anti-human IgG (H + L) secondary antibody (Jackson ImmunoResearch, West Grove, PA) diluted 1:100 in the FACS buffer. The analysis was performed on a FACScan cytometer (Becton and Dickinson) using CellQuest software. Five independent experiments were performed.

Analysis of Cell Proliferation In Vitro by [^{3}H]-Thymidine Incorporation Assay

Inhibition of proliferation of BxPc-3, Capan-1, Colo205, MCF-7, and OZ cells by chiHEA125-Ama was determined by incorporation of [^{3}H]-thymidine. Serial dilutions of chiHEA125-Ama, omalizumab-Ama, and free α-amanitin in the complete medium (ranging from 2×10^{-5} M [18.4 μg/mL] to 6×10^{-13} M [551 fg/mL] with respect to α-amanitin content and corresponding to 5×10^{-6} M [750 μg/mL] to 1.5×10^{-13} M [22.5 pg/mL] IgG) were prepared in a volume of 100 μL in triplicates in a 96-well flat-bottom tissue culture microtiter plate (Techno Plastic Products). To each well, 50 μL cells (5×10^4 per mL) were added. Plates were incubated in a humidified atmosphere at 37°C and 5% CO_2 for 96 hours. Twenty hours before the end of the assay, 1 μCi of [^{3}H]-thymidine was added to each well. Subsequently, the plates were processed with the Tomtec cell harvester (Tomtec, Hamden, CT), and incorporated radioactivity was determined by liquid scintillation counting using a Wallac Betaplate Liquid Scintillation Counter (PerkinElmer Life and Analytical Sciences, Zaventem, Belgium). Data are presented as the percentage of [^{3}H]-thymidine incorporating

cells incubated with different doses of chiHEA125-Ama, omalizumab-Ama, and free α-amanitin for 96 hours. The mean half maximal inhibitory concentration (IC_{50}) for chiHEA125-Ama, omalizumab-Ama, and free α-amanitin was estimated from six independent experiments with MCF-7 cells, four independent experiments with Capan-1, three independent experiments with BxPc-3 and OZ cells, and one independent experiment with Colo205 cells, all performed in triplicate.

In Vivo Human Pancreatic Carcinoma in Mouse Xenograft Model

Female nonobese diabetic/severe combined immunodeficiency mice, 3- to 4-weeks old were purchased from Charles River Laboratories (L'Arbresle, France) and were housed at the animal facility of the German Cancer Research Center. BxPc-3 cells (5×10^6 cells in 100 μL PBS) were transplanted subcutaneously into the right flank of mice (n = 66 mice). Treatment was initiated 10 days later when the BxPc-3 tumors reached a volume of 30–80 mm^3. Experiments were performed with tumors of different volumes. In the first antibody dose escalation experiment, mice bearing BxPc-3 tumors were randomized to four groups and received a single dose of the following: 1) control unconjugated chiHEA125 mAb at a dose of 15 mg/kg of body weight (n = 4 mice); 2) chiHEA125-Ama at a dose of 50 μg/kg with respect to α-amanitin (corresponding to 2.0 mg IgG/kg) (n = 6 mice) (low dose); 3) chiHEA125-Ama, 150 μg/kg with respect to α-amanitin (corresponding to 6.0 mg IgG/kg) (n = 6 mice) (high dose); and 4) chiHEA125-Ama, 300 μg/kg with respect to α-amanitin (corresponding to 12.0 mg IgG/kg) (n = 6 mice) (the highest dose). The doses of chiHEA125-Ama were determined based on the median lethal dose (LD50) value of free α-amanitin in mice (LD50 of free α-amanitin in nude mice is approximately 500 μg/kg after intraperitoneal injection) (29) (J. Anderl, unpublished data). The antibody was administered as a single intraperitoneal injection (day 1). Tumor growth was monitored for 16 days after the initiation of the treatment. Tumor size was measured externally with a caliper every third day. Tumor volume was calculated according to the formula: $V = 4\pi \times a \times b \times c/3$, where a, b, and c are semidiameters in three dimensions. Data are presented as a relative tumor volume increase from the first day of antibody administration. Mice were killed by cervical dislocation at day 25 after tumor cell implantation. Tumors were dissected, weighed, embedded in the Tissue-Tek compound (Sakura Finetek GmbH, Staufen, Germany), snap frozen, and stored at −80°C for further analysis.

In the second antibody dose titration experiment, mice bearing 10-day-old BxPc-3 tumors were randomized to five groups and received two intraperitoneal doses (1 week apart) of the following: 1) control unconjugated chiHEA125 mAb at a dose of 5 mg/kg of body weight (n = 9 mice); 2) chiHEA125-Ama at a dose of 10 μg/kg with respect to α-amanitin (corresponding to 0.4 mg IgG/kg) (n = 8 mice); 3) chiHEA125-Ama, 20 μg/kg with respect to α-amanitin (corresponding to 0.8 mg IgG/kg) (n = 7 mice); 4) chiHEA125-Ama, 50 μg/kg with respect to α-amanitin (corresponding to 2.0 mg IgG/kg) (n = 10 mice); and 5) chiHEA125-Ama, 100 μg/kg with respect to α-amanitin (corresponding to 4.0 mg IgG/kg) (n = 10 mice). Tumor growth was monitored for 16, 40, and 83 days after the initiation of the treatment. The minimal number of mice per group was estimated based on an assumption that the relevant difference is about 20% (using $\alpha = 0.05$ and $\beta < 0.2$). Mice were killed by cervical dislocation at day 16, 40, or 83 after initiation of the treatment.

Mouse experiments were carried out at the animal facility of the German Cancer Research Center following an approval by the Baden-Württemberg animal oversight committee (Regierungspräsidium Karlsruhe, Germany). The number of mice was minimized to comply with guidelines from the Ethical Committee and European Union legislation on animal experiments.

Measurement of Blood Liver Enzymes

Levels of alanine aminotransferase/glutamic-pyruvic transaminase (ALAT/GPT), aspartate aminotransferase/glutamic-oxaloacetic transaminase (ASAT/GOT), gamma-glutamyltransferase (Gamma-GT), alkaline phosphatase (ALP) in the blood of mice treated with chiHEA125-Ama or chiHEA125 (n = 3–5 mice per group) were determined at the Clinical Chemistry Department of the University of Heidelberg. Blood was obtained by heart puncture of anesthetized mice (*S*-ketamine [25 mg/mL Ketanest-S; Pfizer Inc, New York, NY] and xylazine [2% Rompun; Bayer HealthCare, Leverkusen, Germany] in 0.9% NaCl [B. Braun AG, Melsungen, Germany] mixed in 1:4:5 ratio; 250 μL per mouse) at the endpoint of the treatment experiment at day 16 before killing of the mouse.

Morphological Analysis

Immunohistochemistry for Cell Proliferation, Angiogenesis, and Apoptosis. Immunohistochemistry was performed on 6-μm frozen BxPc-3 xenograft tumor tissue sections using the standard avidin–biotin technique with a Vectastain avidin:biotinylated enzyme complex (ABC) Elite kit (Vector Laboratories, Burlingame, CA) or a ZytoChem Plus horseradish peroxidase (HRP) polymer system kit (Zytomed Systems, Berlin, Germany). Briefly, tissue samples were fixed in acetone (Merck) or 4% paraformaldehyde (Merck) followed by incubation with 20% normal goat or rabbit serum in PBS to block unspecific binding of antibodies. After incubation with primary mAb and washing with PBS three times, tissue samples were incubated with biotinylated secondary antibody or with a HRP mouse/rabbit polymer system. Diaminobenzidin (DAB) (Invitrogen) or 3-amino-9-ethylcarbazole (AEC) (Zytomed Systems) were used as chromogens. The following primary antibodies were used: rat anti-mouse CD31 mAb (1:100 dilution) (BD Pharmingen, Heidelberg, Germany) for detection of endothelial cells, mouse anti-human Ki-67 antibody (1:100 dilution) (Dako, Glostrup, Denmark) as a marker of tumor cell proliferation, home-made mouse anti-human EpCAM (HEA125, IgG_1) mAb (1:100 dilution), home-made mouse anti-human CD24 (SWA11, IgG_{2A}) mAb (1:200 dilution), rabbit polyclonal anti-human CD44 antibody (1:50 dilution) (Abcam, Cambridge, UK), and rabbit polyclonal anti-human CD133 antibody (1:50 dilution) (Abcam) as cancer stem cell markers. Biotinylated goat anti-mouse IgG, biotinylated goat anti-rabbit, and biotinylated rabbit anti-rat IgG (1:200 dilution) (Vector Laboratories) were used as secondary antibodies. For double immunofluorescence staining, goat anti-mouse IgG conjugated to Alexa 488 or goat anti-rabbit Alexa 594 IgG (1:400

dilution) (Invitrogen) were used as secondary antibodies. Omission of primary antibody was used as a negative control. Apoptosis was detected by staining for active caspase 3 with rabbit anti-human polyclonal antibody (1:100 dilution) (R&D Systems, Abingdon, UK). Tissue stainings were examined at ×400 and ×100 magnification with a Leica DMRB microscope (Leica Microsystems, Wetzlar, Germany). Images were captured with a SPOT Flex digital color camera (Diagnostic Instruments Inc, Sterling Heights, MI) and analyzed with SPOT Advanced version 4.6 software. Ki-67-positive and active caspase 3–positive cells were counted under ×400 magnification in 10 random fields of vision (0.089 mm^2) per slide (n = 3–4 mice per group, unless otherwise specified). Data in each treatment group are presented as the mean percentage of Ki-67-positive or active caspase 3–positive cells per total tumor cellular mass counted in the same fields of vision. CD31-positive blood vessels were counted under ×100 magnification in 10 random fields of vision (1.46 mm^2) per slide (n = 3–4 mice per group, unless otherwise specified). Data in each treatment group are presented as the mean number of CD31-positive blood vessels per mm^2 of tumor tissue. The number of CD31-positive blood vessels, proliferating and apoptotic tumor cells was counted by an investigator who was blinded to the type of treatment received by the mice.

Terminal Deoxynucleotidyl Transferase dUTP Nick End Labeling (TUNEL) Assay. To quantify the number of apoptotic cells in 6-μm cryosections of BxPc-3 xenograft tumors treated with chiHEA125-Ama or control unconjugated chiHEA125 mAb, we performed a TUNEL assay with TACS TdT in situ apoptosis detection kit (R&D Systems) according to the manufacturer's recommendations and modified by signal enhancement using a Vectastain ABC Elite kit (Vector Laboratories) and color development using a DAB kit (Invitrogen). TUNEL-positive cells were counted under ×400 magnification in 10 random fields of vision (0.089 mm^2) per slide (n = 3–4 mice per group, unless otherwise specified). Data in each treatment group are presented as the mean percentage of TUNEL-positive cells per total tumor cellular mass counted in the same fields of vision. The number of apoptotic tumor cells was counted by an investigator who was blinded to the type of treatment received by the mice.

Statistical Analysis

Data were analyzed using Predictive Analytics Software (PASW) Statistics 18, version 18.0.2 (SPSS Inc, Chicago, IL). In vitro and in vivo data are presented as mean values with 95% confidence intervals (CIs). A two-sided Student's *t* test was used to evaluate the difference between two groups. If multiple comparisons were performed, a Bonferroni–Holms correction was applied. *P* values less than .05 were considered statistically significant.

Results

Effect of α-Amanitin Conjugation on Binding of chiHEA125 to EpCAM

ChiHEA125-Ama was produced by covalent conjugation of α-amanitin from *Amanita phalloides* mushrooms to the lysine residues of the chiHEA125 mAb using glutaric anhydride and dicyclohexyl carbodiimide cross-linking chemistry (Figure 1, A). An

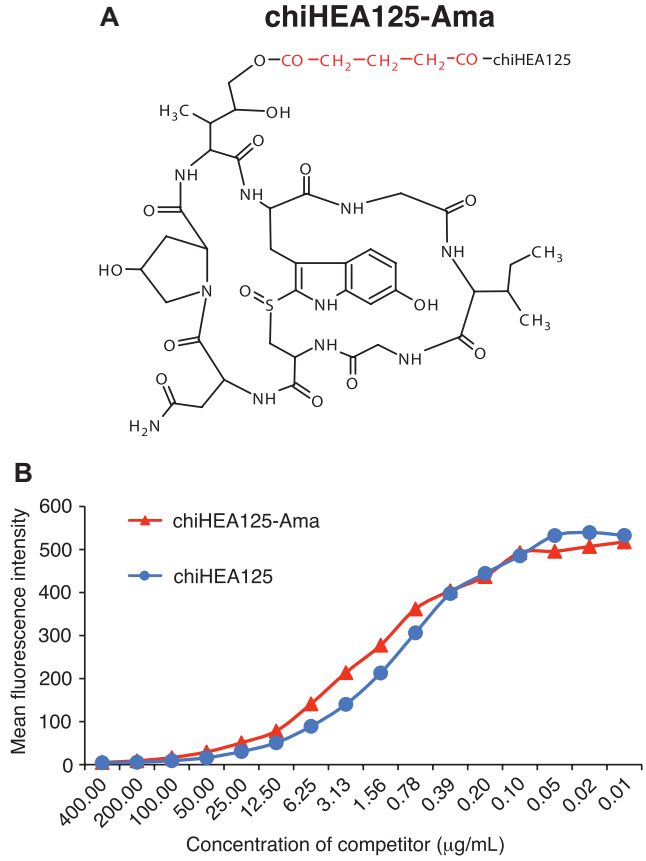

Figure 1. Structure and binding of α-amanitin-conjugated chiHEA125 monoclonal antibody to epithelial cell adhesion molecule (EpCAM). The antibody–drug conjugate chiHEA125-Ama was generated by a chemical cross-linking of a toxin α-amanitin with chiHEA125, a chimerized anti-EpCAM monoclonal antibody using glutarate as a linker. Binding of chiHEA125-Ama vs nonconjugated chiHEA125 antibody to EpCAM-expressing Colo205 colon cancer cells was analyzed in a binding competition assay by flow cytometry. **A**) Structure of chiHEA125-Ama and α-amanitin conjugation site for chiHEA125 immunoglobulin G (IgG). **B**) Binding of α-amanitin-conjugated chiHEA125 IgG (chiHEA125-Ama) and parental nonconjugated chiHEA125 IgG to the target antigen EpCAM using Colo205 cells. Cells (2×10^7 cells per mL) were incubated with serial dilutions of chiHEA125-Ama or chiHEA125 ranging from 400 μg/mL to 10 ng/mL of IgG at final dilution and analyzed by flow cytometry. Mean fluorescence intensity was quantified using CellQuest software. Results are representatives of two independent experiments performed in triplicate. Ama = α-amanitin.

α-amanitin:antibody ratio of 4:1 to 8:1 was determined by spectrophotometric analysis of increased ultraviolett absorbance at 310 nm of the chiHEA125-Ama compared with the nonconjugated chiHEA125 mAb (Supplementary Figure 2, A, available online). Size-exclusion chromatography revealed low amounts (<3%) of aggregated or cross-linked IgG protein after α-amanitin conjugation (Supplementary Figure 2, B, available online). According to the immunoblot analysis using a polyclonal anti-amanitin antiserum, α-amanitin was conjugated equally to the heavy and light chains of chiHEA125 mAb (Supplementary Figure 2, C and D, available online). We further analyzed whether the α-amanitin payload affected chiHEA125-Ama binding to the target antigen EpCAM. Competition of binding to target Colo205 cancer cells with increasing amounts of chiHEA125-Ama or unmodified chiHEA125 antibody revealed a comparable binding strength as

evidenced by the flow cytometry analysis of mean fluorescence intensity at all concentrations of the competitor (Figure 1, B). Therefore, conjugation of 4–8 α-amanitin molecules per chiHEA125 antibody did not substantially alter the affinity of chiHEA125 to EpCAM antigen.

Effect of chiHEA125-Ama on Proliferation of Multiple Carcinoma Cell Lines In Vitro

Expression of EpCAM in all tested cancer cell lines was determined by indirect flow cytometry (Supplementary Figure 3, available online). Using a [^{3}H]-thymidine incorporation assay, we found that chiHEA125-Ama strongly inhibited proliferation of EpCAM-expressing Colo205 cancer cells at picomolar concentrations compared with control α-amanitin-conjugated anti-human IgE mAb (omalizumab-Ama) or an unconjugated α-amanitin (Figure 2, A and Table 1). Similar antiproliferative effects of chiHEA125-Ama were observed in other EpCAM-expressing cancer cell lines (Figure 2, B–E; Table 1; and Supplementary Figure 3, available online). Proliferation of human OZ bile duct carcinoma cell line, Capan-1, and BxPc-3 pancreatic cancer cell lines as well as MCF-7 breast cancer cell line was strongly inhibited by concentrations of chiHEA125-Ama up to 10^4-fold lower than the control omalizumab-Ama or α-amanitin alone (chiHEA125-Ama vs free α-amanitin: OZ cells, mean IC_{50} = 8.7×10^{-11} M [95% CI = -5.5×10^{-11} to 2.3×10^{-10} M] vs 5.1×10^{-07} M [95% CI = 7.2×10^{-08} to 9.6×10^{-07} M]; Capan-1 cells, mean IC_{50} = 2.1×10^{-11} M [95% CI = 2.7×10^{-12} to 3.9×10^{-11} M] vs 1.9×10^{-07} M [95% CI = 7.8×10^{-08} to 3.1×10^{-07} M]; BxPc-3 cells, mean IC_{50} = 2.5×10^{-10} M [95% CI = 3.4×10^{-11} to 4.6×10^{-10} M] vs 2.5×10^{-08} M [95% CI = -3.01×10^{-09} to 5.4×10^{-08} M]; MCF-7 cells, mean IC_{50} = 5.4×10^{-12} M [95% CI = -1.5×10^{-12} to 1.2×10^{-11} M] vs 5.8×10^{-08} M [95% CI = 3.6×10^{-08} to 8.09×10^{-08} M]) (Figure 2, and Table 1). The unconjugated chiHEA125 mAb had no effect on proliferation of cancer cell lines (data not shown).

Effect of Single Injection of chiHEA125-Ama on Growth of Human Pancreatic Carcinoma in a Mouse Xenograft Model

Next, we investigated the in vivo antitumor activity of chiHEA125-Ama in an experimental human BxPc-3 pancreatic cancer model, induced by injecting BxPc-3 cancer cells subcutaneously into the right flank of female nonobese diabetic/severe combined immune deficiency mice. This cell line was chosen because this well established in vivo model resembles the growth of human pancreatic cancer containing beside the carcinoma cells abundant tumor stroma (37). In a dose escalation experiment, chiHEA125-Ama was administered to BxPc-3 pancreatic xenograft tumor–bearing mice as a single intraperitoneal injection. Mice bearing 10-day-old xenografts received chiHEA125-Ama at the dose of 50, 150, or 300 μg with respect to α-amanitin per kg of mouse body weight (corresponding to 2.0, 6.0, or 12.0 mg IgG/kg) (n = 6 mice per group). Control mice received unconjugated chiHEA125 mAb at a dose of 15 mg/kg of body weight (n = 4 mice). The chiHEA125-Ama at the dose of 50 μg/kg showed strong inhibition of tumor growth (n = 6 mice) (Figure 3, A). All tumors responded to the chiHEA125-Ama treatment, and tumor volume regressed dramatically starting from day 7 after the chiHEA125-Ama administration.

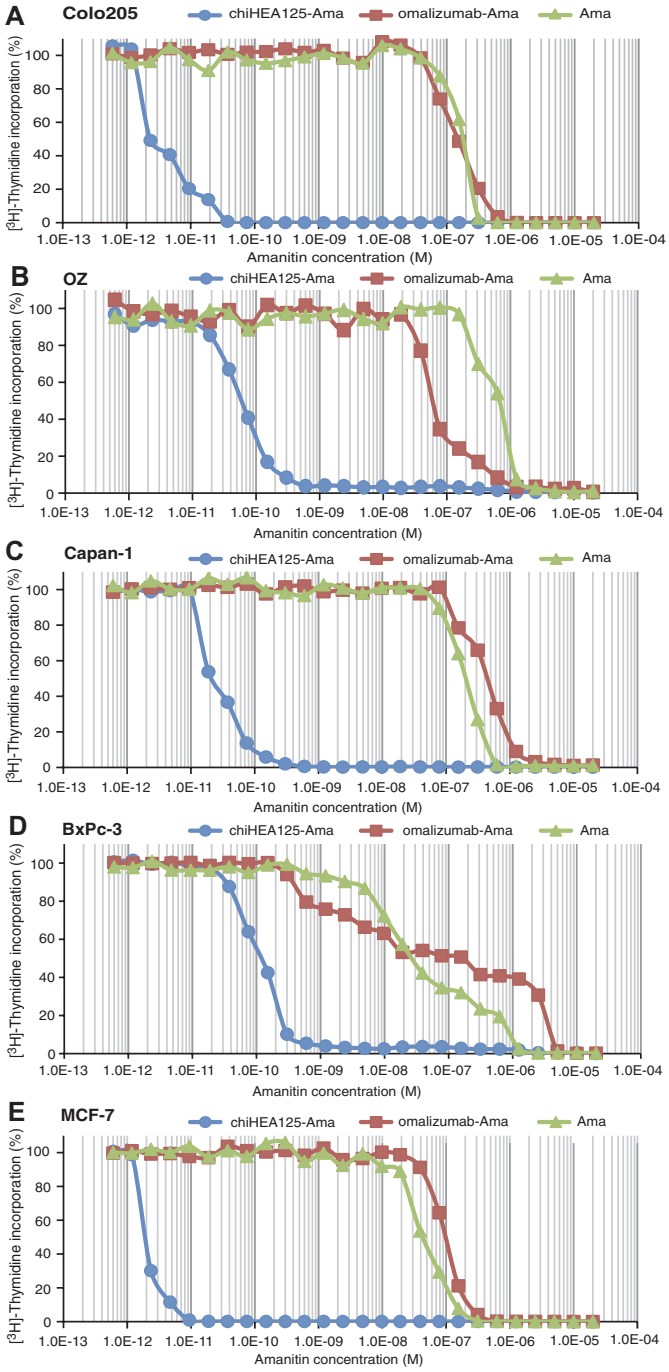

Figure 2. Effect of chiHEA125-Ama on proliferation of multiple carcinoma cell lines in vitro. Effect of chiHEA125-Ama on cancer cells proliferation was analyzed by a standard [^{3}H]-thymidine incorporation assay. ChiHEA125-Ama, control α-amanitin-conjugated anti-human IgE monoclonal antibody (omalizumab-Ama) and unconjugated α-amanitin were added to cultured carcinoma cells at the indicated doses and the percentage of [^{3}H]-thymidine incorporating cells was evaluated after 96 hours of incubation. The logarithmic *x*-axis shows the concentrations of chiHEA125-Ama, omalizumab-Ama, and free α-amanitin in a scale. **A**) Human colorectal cancer cell line Colo205. **B**) Human bile duct cancer cell line OZ. **C**) Human pancreatic cell line Capan-1. **D**) Human pancreatic cell line BxPc-3. **E**) Human breast cancer cell line MCF-7. Results are representatives of six independent experiments with MCF-7 cells, four independent experiments with Capan-1, three independent experiments with BxPc-3 and OZ cells, and one independent experiment with Colo205 cells, all performed in triplicate. Ama = α-amanitin.

Table 1. Effect of chiHEA125-Ama and free α-amanitin on cell proliferation*

Cancer type, cell line	IC_{50}, mean (95% CI)		Ratio, amanitin:ADC†
	chiHEA125-Ama	α-Amanitin	
Colorectal, Colo205	2×10^{-12} M‡	2×10^{-07} M‡	100 000
Bile duct, OZ	8.7×10^{-11} M (-5.5×10^{-11} to 2.3×10^{-10} M)	5.1×10^{-07} M (7.2×10^{-08} to 9.6×10^{-07} M)	5862
Pancreatic, Capan-1	2.1×10^{-11} M (2.7×10^{-12} to 3.9×10^{-11} M)	1.9×10^{-07} M (7.8×10^{-08} to 3.1×10^{-07} M)	9048
Pancreatic, BxPc-3	2.5×10^{-10} M (3.4×10^{-11} to 4.6×10^{-10} M)	2.5×10^{-08} M (-3.01×10^{-09} to 5.4×10^{-08} M)	100
Breast, MCF-7	5.4×10^{-12} M (-1.5×10^{-12} to 1.2×10^{-11} M)	5.8×10^{-08} M (3.6×10^{-08} to 8.09×10^{-08} M)	10741

* Cells were treated with chiHEA125-Ama or free α-amanitin at concentrations ranging from 2×10^{-5} M (18.4 μg/mL) to 6×10^{-13} M (551 fg/mL) with respect to α-amanitin content (corresponding to 5×10^{-6} M [750 μg/mL] to 1.5×10^{-13} M [22.5 pg/mL] IgG), and half maximal inhibitory concentrations (IC_{50}) were estimated to determine the antiproliferative activity. Data are presented from six independent experiments with MCF-7 cells, four independent experiments with Capan-1, three independent experiments with BxPc-3 and OZ cells, and one independent experiment with Colo205 cells. ADC = an antibody–drug conjugate; CI = confidence interval.

† The ratio signifies a magnitude of free α-amanitin doses required to reach equal IC_{50} concentrations with chiHEA125-Ama.

‡ No 95% CIs were obtained from one independent experiment.

In contrast, the control mice (n = 4), which received unconjugated chiHEA125 mAb (15 mg/kg), showed an increase in tumor volume by approximately 880% after 16 days of antibody injection (chiHEA125 vs chiHEA125-Ama, mean relative increase in tumor volume on day 16 = 884% vs −79%, difference = 963%, 95% CI = 582% to 1344%, $P = .019$) (Figure 3, A and B, and Supplementary Figure 4, A, available online). In 3 (50%) of 6 mice, complete tumor regression was observed 16 days after the administration of chiHEA125-Ama.

BxPc-3 tumors that were visually detectable after chiHEA125-Ama treatment on day 16 were then analyzed by immunohistochemistry for cell proliferation (n = 3–4 mice per group) and apoptosis (n = 3–4 mice per group). The chiHEA125-Ama treatment (50 μg/kg) reduced tumor cell proliferation, which was evident from a decreased percentage of Ki-67-positive cells compared with tumors from chiHEA125-treated mice (chiHEA125 vs chiHEA125-Ama, mean percentage of Ki-67-positive cells = 56% vs 40%, difference = 16%, 95% CI = 10% to 22%, $P = .0014$) (Figure 3, C and Supplementary Figure 4, B, available online). In addition, compared with the controls, the percentage of active caspase 3–positive apoptotic cells slightly increased in BxPc-3 tumors treated with chiHEA125-Ama, but the increase was not statistically significant (chiHEA125 vs chiHEA125-Ama, mean percentage of active caspase 3–positive cells = 1.97% vs 3%, difference = −1.03%, 95% CI = −3% to 0.95%, $P = .24$) (Figure 3, D and Supplementary Figure 4, B, available online). The percentage of TUNEL-positive apoptotic cells was also not statistically significant (chiHEA125 vs chiHEA125-Ama: mean = 1.4% vs 1.6%, difference = −0.2%, 95% CI = −1.2% to 0.9%, $P = .74$) (Figure 3, E).

BxPc-3 tumor–bearing mice well tolerated the treatment with chiHEA125-Ama at the dose of 50 μg/kg. Their body weight was stable throughout the experiment (data not shown). The analysis of blood liver enzymes (ALAT/GPT, ASAT/GOT, Gamma-GT, ALP) did not reveal any substantial difference between the mice that received chiHEA125-Ama and the control mice treated with an unconjugated chiHEA125 mAb (data not shown). In contrast, 2 (30%) of 6 and 3 (50%) of 6 mice treated with chiHEA125-Ama at high doses of 150 or 300 μg/kg, respectively, exhibited signs of pronounced liver toxicity evidenced by severe loss of body weight and gross liver morphology. Therefore, mice treated with these high doses of chiHEA125-Ama were excluded from further analysis.

Effect of Two Doses of chiHEA125-Ama on Growth of Human Pancreatic Carcinoma in Mouse Xenograft Model

For dose titration of chiHEA125-Ama, BxPc-3 tumor–bearing mice were treated with two injections of chiHEA125-Ama, administered 1 week apart, at doses of 10, 20, 50, and 100 μg/kg with respect to α-amanitin (corresponding to 0.4, 0.8, 2.0, and 4.0 mg IgG/kg) (n = 8, 7, 10, and 10 mice per group, respectively). Tumor growth was monitored for the following 16 days. BxPc-3 tumor-bearing mice well tolerated the treatment with all doses of chiHEA125-Ama. At the endpoint of the treatment, tumors were no longer detectable in six (60%) of 10 and nine (90%) of 10 of mice treated with chiHEA125-Ama at a dose of 50 and 100 μg/kg, respectively (Figure 4, A and Supplementary Figure 5, A, available online). Two injections of chiHEA125-Ama at doses of 10 or 20 μg/kg showed non-statistically significant inhibition of BxPc-3 tumor growth compared with the control mice treated with unconjugated chiHEA125 IgG (5 mg/kg) (n = 9 mice) (relative tumor volume increase on day 16, chiHEA125 vs chiHEA125-Ama 10 μg/kg, mean = 738% vs 663%, difference = 75%, 95% CI = −230% to 381%, $P = .98$; chiHEA125 vs chiHEA125-Ama 20 μg/kg, mean = 738% vs 454%, difference = 284%, 95% CI = −26% to 595%, $P = .81$), whereas higher doses showed statistically significant inhibition of tumor growth (chiHEA125 vs chiHEA125-Ama 50 μg/kg, mean = 738% vs −45%, difference = 783%, 95% CI = 550% to 1015%, $P < .001$; chiHEA125 vs chiHEA125-Ama 100 μg/kg, mean = 738% vs −89%, difference = 827%, 95% CI = 602 to 1051%, $P < .001$) (Figure 4, A, and Supplementary Figure 5, A). All P values were corrected for multiple comparisons using a Bonferroni–Holms correction.

BxPc-3 tumors that were visually detectable after chiHEA125-Ama treatment on day 16 were then analyzed by immunohistochemistry for tumor cell proliferation and apoptosis. In all groups, chiHEA125-Ama treatment reduced tumor cell proliferation in a dose-dependent manner (percentage of Ki-67-positive cells: chiHEA125 vs chiHEA125-Ama 10 μg/kg, mean = 49% vs 41%, difference = 8%, 95% CI = 0.22% to 16.57%, $P = .045$; chiHEA125 vs chiHEA125-Ama 20 μg/kg, mean = 49% vs 38%, difference = 11%, 95% CI = 4% to 19%, $P = .006$; chiHEA125 vs chiHEA125-Ama 50 μg/kg, mean = 49% vs 33%, difference = 16%, 95% CI = 7% to 25%, $P = .005$; chiHEA125 vs chiHEA125-Ama 100 μg/kg, mean = 49% vs 23%, difference = 26%, 95% CIs and P value could not be

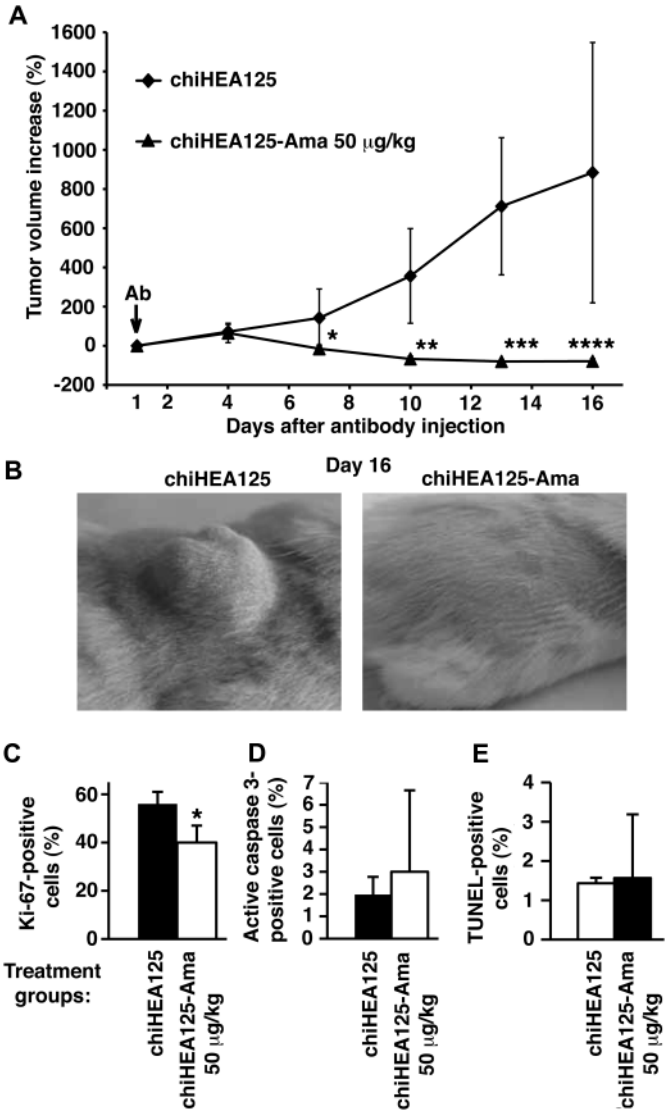

Figure 3. Efficiency of a single dose of chiHEA125-Ama on BxPc-3 tumor growth in vivo. Mice bearing 10-day-old xenograft BxPc-3 pancreatic carcinomas received a single intraperitoneal injection of chiHEA125-Ama at a dose of 50 μg/kg with respect to α-amanitin (corresponding to 2.0 mg IgG/kg) (n = 6 mice). Control mice received unconjugated chiHEA125 monoclonal antibody (15 mg/kg) (n = 4 mice). **A**) Tumor growth was measured every third day, and data are presented as a relative tumor volume increase starting from treatment initiation. **Error bars** correspond to 95% confidence intervals. * $P = .04$, ** $P = .01$, *** $P = .005$, **** $P = .019$; calculated using a two-sided Student's *t* test. An **arrow** indicates time of chiHEA125 or chiHEA125-Ama administration. **B**) Representative BxPc-3 tumors at the endpoint of the treatment, day 16. Magnification = ×2.5. **C**) Proliferation of tumor cells in BxPc-3 tumors that were visually detectable after chiHEA125-Ama treatment was investigated by immunohistochemistry for Ki-67 on day 16. Ki-67-positive cells were counted under ×400 magnification in 10 random fields of vision (n = 3–4 mice per group). Data are presented as the percentage of Ki-67-positive cells per total tumor cellular mass. * $P = .0014$; calculated using a two-sided Student's *t* test. **Error bars** correspond to upper 95% confidence intervals. **D**) Analysis of apoptosis in BxPc-3 tumors that were visually detectable after chiHEA125-Ama treatment using immunohistochemical staining for active caspase 3. Error bars correspond to upper 95% confidence intervals. **E**) Analysis of apoptosis in BxPc-3 tumors using a Terminal Deoxynucleotidyl Transferase dUTP Nick End Labeling (TUNEL) assay. Active caspase 3–positive and TUNEL-positive cells were counted under ×400 magnification in 10 random fields of vision (n = 3–4 mice per group). Data are presented as the percentage of positive cells per total tumor cellular mass. **Error bars** correspond to upper 95% confidence intervals. Ama = α-amanitin.

obtained from one detectable tumor) (Figure 4, B). Increased apoptosis was also observed in tumors (percentage of active caspase 3–positive cells, chiHEA125 vs chiHEA125-Ama 10 μg/kg, mean = 1.2% vs 2.5%, difference = −1.3%, 95% CI = −1.8% to −0.7%, $P < .001$; chiHEA125 vs chiHEA125-Ama 20 μg/kg, mean = 1.2% vs 2.5%, difference = −1.3%, 95% CI = −2.4% to −0.09%, $P = .036$; chiHEA125 vs chiHEA125-Ama 50 μg/kg, mean = 1.2% vs 5.3%, difference = −4.1%, 95% CI = −8.1% to 0.09%, $P = .047$; chiHEA125 vs chiHEA125-Ama 100 μg/kg, mean = 1.2% vs 15.6%, difference = 14.4%, no 95% CIs and *P* value could be obtained from one detectable tumor) (Figure 4, C). Apoptosis was most pronounced in tumors treated with chiHEA125-Ama at a dose of 100 μg/kg, where, in addition to the areas with the average distribution of apoptotic cells within the tumor (Figure 4, D), multiple areas with almost 50%–70% of active caspase 3–positive tumor cells were observed (Figure 4, E).

We further monitored relapse of tumor growth in mice without palpable tumors at day 16 during 40 days of observation after the initiation of treatment (n = 5 mice per group). In the group treated with 50-μg/kg chiHEA125-Ama (n = 5 mice), the earliest relapse of tumor growth was observed 21–24 days after the last chiHEA125-Ama injection (Figure 5, A, and Supplementary Figure 5, B, available online) and found in four (80%) of five mice at day 40. Much more effective in preventing BxPc-3 tumor relapse was treatment with the higher dose of chiHEA125-Ama (100 μg/kg) (n = 5 mice). Here, recurrence of tumor growth was detectable as early as day 28 after the last chiHEA125-Ama injection and was evident in only two (40%) of five mice (Figure 5, B and Supplementary Figure 5, C, available online). Excitingly, 40% of the mice in this group showed complete tumor eradication. These mice (two of five) did not develop recurrent tumors even after 83 days following the initiation of the treatment.

The microscopic analysis of the recurrent tumors on day 40 revealed that the percentage of apoptotic cells was still high and the percentage of Ki-67-positive tumor cells was similar to that at day 16 (percentage of active caspase 3–positive cells at day 40 in chiHEA125-Ama 50 μg/kg: mean = 4%, 95% CI = 2.99% to 5.01%; percentage of Ki-67-positive cells at day 40 in chiHEA125-Ama 50 μg/kg: mean = 33%, 95% CI = 24% to 42%) (Figure 5, C and D compared with Figure 4, B and C). The recurrent tumors were EpCAM positive at day 40 (data not shown) as well as at day 83 (Supplementary Figure 5, D, available online) after the initiation of chiHEA125-Ama treatment. To exclude a possibility that chiHEA125-Ama treatment would select for aggressive cancer cells with cancer stem cell characteristics, we analyzed recurrent tumors for cancer stem cell marker expressions. An expression of CD133 molecule, a marker of cancer stem cells, could not be detected in recurrent tumors neither at day 40 nor at day 83 after treatment (data not shown). In BxPc-3 xenografts, treatment with chiHEA125-Ama did not change the proportion of the tumor cells with $CD44^+/CD24^+$ phenotype, which was recently attributed to cancer stem cells (14) (data not shown).

Effect of chiHEA125-Ama Treatment on Tumor Angiogenesis

Next, we investigated whether antitumor effects of chiHEA125-Ama were because of inhibition of tumor angiogenesis.

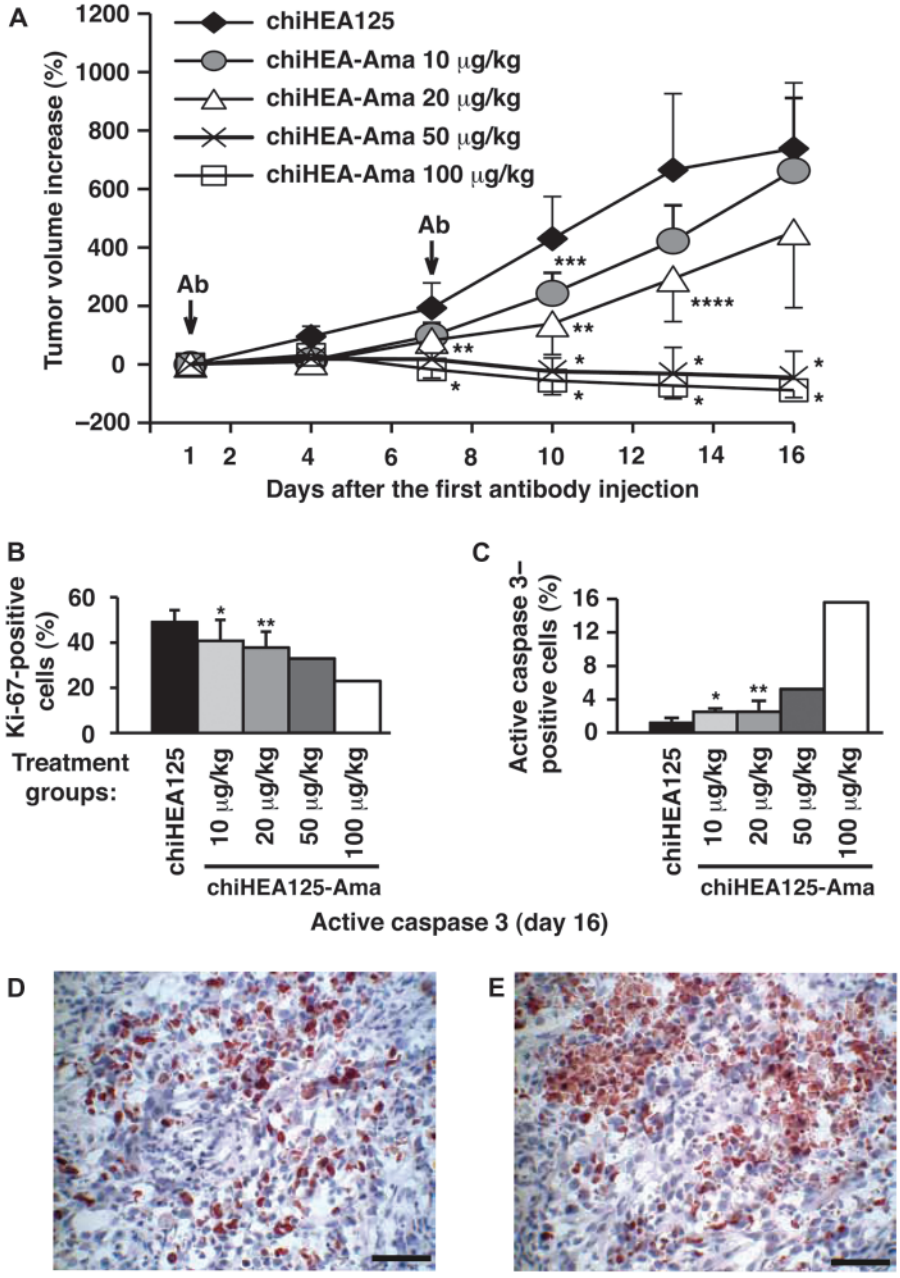

Figure 4. Efficiency of two doses of chiHEA125-Ama on BxPc-3 tumor growth in vivo. Dose titration experiments with two intraperitoneal injections of chiHEA125-Ama, administered 1 week apart. Mice bearing 10-day-old xenograft BxPc-3 tumors received intraperitoneal injections of chiHEA125-Ama (10, 20, 50, and 100 μg/kg, corresponding to 0.4, 0.8, 2.0, or 4.0 mg IgG/kg, respectively; n = 8, 7, 10, 10 mice per group, respectively) or control unconjugated chiHEA125 monoclonal antibody (5 mg/kg) (n = 9 mice). **A**) Tumor growth was measured every third day, and data are presented as a relative tumor volume increase after the first antibody injection. **Error bars** correspond to upper or lower 95% confidence intervals. * $P < .001$, ** $P = .001$, *** $P = .019$, **** $P = .013$ (two-sided Student's *t* test). **Arrows** indicate time of chiHEA125 or chiHEA125-Ama (antibody) administration. **B**) Effects of different doses of chiHEA125-Ama (10 μg/kg, n = 5 mice; 20 μg/kg, n = 5 mice; 50 μg/kg, n = 2 mice; and 100 μg/kg, n = 1 mouse, corresponding to 0.4, 0.8, 2.0, or 4.0 mg IgG/kg, respectively) and unconjugated chiHEA125 antibodies (5 mg/kg, n = 5 mice) on cell proliferation in BxPc-3 tumors that were visually detectable after chiHEA125-Ama treatment were analyzed by immunohistochemistry on day 16. **C**) Effects of different doses of chiHEA125-Ama (10 μg/kg, n = 5 mice; 20 μg/kg, n = 5 mice; 50 μg/kg, n = 2 mice; and 100 μg/kg, n = 1 mouse, corresponding to 0.4, 0.8, 2.0, or 4.0 mg IgG/kg, respectively) and unconjugated chiHEA125 Abs (5 mg/kg, n = 5 mice) on tumor cell apoptosis in BxPc-3 tumors that were visually detectable after chiHEA125-Ama treatment were analyzed by immunohistochemistry on day 16. Ki-67-positive or active caspase 3–positive cells were counted under ×400 magnification in 10 random fields of vision. Data are presented as the percentage of positive cells per total tumor cellular mass. * $P = .045$, ** $P = .006$ (for active caspase 3, * $P < .001$ and ** $P = .036$) (two-sided Student's *t* test). **Error bars** correspond to upper 95% confidence intervals. **D**) Representative images of active caspase 3 staining of BxPc-3 tumor treated with two injections of chiHEA125-Ama at a dose of 100 μg/kg at the endpoint of the experiment at day 16. **E**) There were areas within the tumor with almost 50%–70% of active caspase 3–positive tumor cells (**red**). Scale bar = 50 μm. Ama = α-amanitin.

Immunohistochemical staining of CD31, a marker of endothelial cells, did not reveal any difference in the density of CD31-positive blood vessels between BxPc-3 tumors treated with a single injection of chiHEA125-Ama (50 μg/kg with respect to α-amanitin) and the control tumors treated with an unconjugated chiHEA125 mAb (15 mg/kg) (chiHEA125 vs chiHEA125-Ama, number of CD31-positive blood vessels per mm^2 of tumor tissue: mean = 58 vs 61, difference = −3, 95% CI = −15.7 to 9.89, $P = .58$) (Figure 6, A). Even two doses of chiHEA125-Ama, given a week apart, did not affect angiogenesis in BxPc-3 tumors at day 16 (the number of CD31-positive blood vessels per mm^2 of tumor tissue: chiHEA125 vs chiHEA125-Ama 10 μg/kg, mean = 50 vs 49.4, difference = 0.6, 95% CI = −7.8 to 9.1, $P = .09$; chiHEA125 vs chiHEA125-Ama 20 μg/kg, mean = 50 vs 59, difference = −9, 95% CI = −17 to 0.02, $P = .37$; chiHEA125 vs chiHEA125-Ama 50 μg/kg, mean = 50 vs 55, difference = −5, 95% CI = −46 to −36, $P = .44$; chiHEA125 vs chiHEA125-Ama 100 μg/kg, mean = 50 vs 60, difference = −10, 95% CIs and *P* value could not be obtained from one detectable tumor) (Figure 6, B), which indicates that tumor regression was because of specific targeting of EpCAM-positive tumor cells by the chiHEA125-Ama. As BxPc-3 tumors regressed after chiHEA125-Ama treatment, the density of CD31-positive blood vessels also decreased at day 40 after treatment (chiHEA125-Ama 50 μg/kg, the number of CD31-positive blood vessels per mm^2 of tumor tissue at day 40: mean = 35, 95% CI = 30 to 40) (Figure 6, C). Recurrence of BxPc-3 tumors was associated with a slight increase in CD31-positive vessel density at day 83 compared with that at day 40 (data not shown).

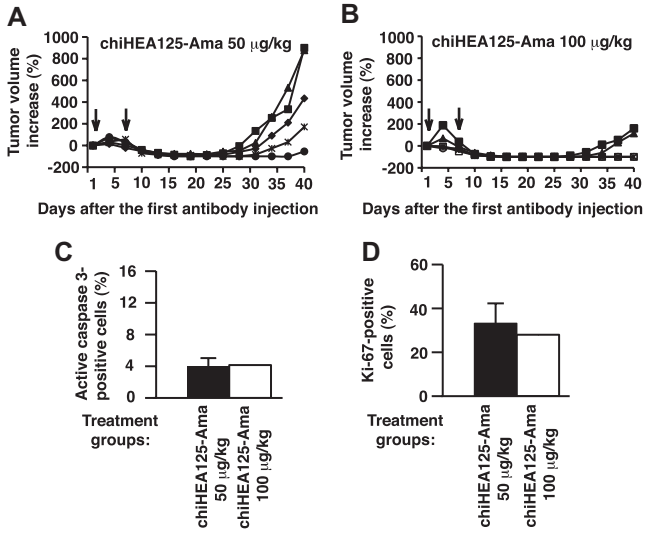

Figure 5. Long-term efficiency of two injections of chiHEA125-Ama at doses of 50 and 100 μg/kg of α-amanitin on BxPc-3 tumor growth in vivo. BxPc-3 tumor growth recurrence after two intraperitoneal injections of chiHEA125-Ama, administered 1 week apart, was monitored for a period of 40 days after the first chiHEA125-Ama injection. **A**) Mice bearing 10-day-old xenograft BxPc-3 tumors (n = 5 mice) received two intraperitoneal injections of chiHEA125-Ama at a dose of 50 μg/kg, corresponding to 2.0 mg IgG/kg. **B**) Mice bearing 10-day-old xenograft BxPc-3 tumors (n = 5 mice) received two intraperitoneal injections of chiHEA125-Ama at a dose of 100 μg/kg, corresponding to 4.0 mg IgG/kg. Tumor growth was measured every third day. The relative tumor volume increase of individual tumors is shown. **Arrows** indicate time of chiHEA125-Ama administration. **C**) Apoptosis was analyzed by immunohistochemistry at day 40 after the first chiHEA125-Ama injection (chiHEA125-Ama 50 μg/kg n = 5 mice, chiHEA125-Ama 100 μg/kg n = 2 mice). **D**) Tumor cell proliferation was analyzed by immunohistochemistry at day 40 after the first chiHEA125-Ama injection (chiHEA125-Ama 50 μg/kg n = 5 mice, chiHEA125-Ama 100 μg/kg n = 2 mice). Active caspase 3–positive or Ki-67-positive cells were counted under ×400 magnification in 10 random fields of vision. Data are presented as the percentage of positive cells per total tumor cellular mass. **Error bars** correspond to upper 95% confidence intervals. Ama = α-amanitin.

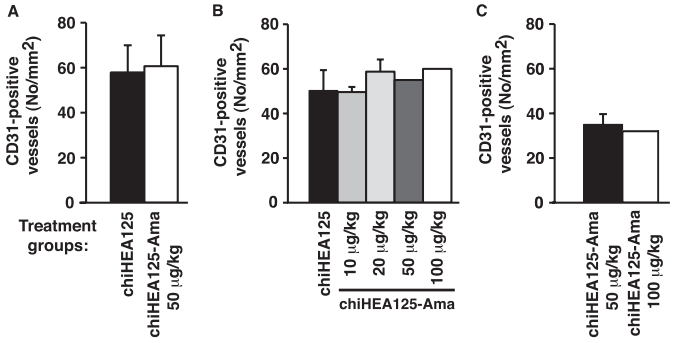

Figure 6. Effects chiHEA125-Ama treatment on blood vessel density in BxPc-3 tumor xenografts. The density of blood vessels in BxPc-3 tumors was analyzed by immunohistochemistry using cluster of differentiation 31 (CD31) as a marker of endothelial cells. CD31-positive blood vessels were counted in 10 random fields of vision ×100 magnification. Data in each treatment group are presented as the mean number of CD31-positive blood vessels per mm² of tumor tissue. **A**) Effect of a single dose of chiHEA125-Ama (50 μg/kg) (n = 4 mice) and unconjugated chiHEA125 monoclonal antibody (mAb) (15 mg/kg) (n = 3 mice) on angiogenesis in BxPc-3 tumors was determined at the endpoint at day 16. **Error bars** correspond to upper 95% confidence intervals. **B**) Effects of two injections of different doses of chiHEA125-Ama (10 μg/kg, n = 5 mice; 20 μg/kg, n = 4 mice; 50 μg/kg, n = 2 mice; and 100 μg/kg, n = 1 mouse) and unconjugated chiHEA125 mAb (5 mg/kg, n = 4 mice), administered 1 week apart, on BxPc-3 tumor angiogenesis evaluated at day 16 after the first antibody injection. **Error bars** correspond to upper 95% confidence intervals. **C**) The density of CD31-positive blood vessels in BxPc-3 tumors that received chiHEA125-Ama at doses of 50 μg/kg (n = 4 mice) or 100 μg/kg (n = 2 mice) evaluated at day 40 after the first antibody injection. **Error bars** correspond to upper 95% confidence intervals. Ama = α-amanitin.

Discussion

In this study, we show that a novel ADC consisting of α-amanitin conjugated to a chimerized anti-EpCAM mAb (chiHEA125-Ama) has a potent antitumor activity against experimental pancreatic carcinoma in vitro and in vivo. In vitro, chiHEA125-Ama exhibited cogent antiproliferative activity against pancreatic, colorectal, breast, and bile duct cancer cell lines. A single dose of chiHEA125-Ama elicited a strong inhibition of subcutaneous BxPc-3 pancreatic xenograft tumor growth compared with BxPc-3 tumors treated with control unconjugated chiHEA125 mAb. Two injections of chiHEA125-Ama at doses 50 or 100 μg/kg with respect to α-amanitin, administered 1 week apart, showed complete tumor regression in 60% and 90% of mice, respectively, compared with chiHEA125, during the observation period of 16 days. These two doses of chiHEA125-Ama effectively controlled BxPc-3 tumor recurrence for a period of 3–4 weeks. In addition, 40% mice treated with two higher doses of chiHEA125-Ama (100 μg/kg with respect to α-amanitin) did not develop recurrent tumors even after 83 days following the initiation of the treatment. Increased apoptosis and reduced tumor cell proliferation were observed in tumors treated with chiHEA125-Ama. Importantly, mice well tolerated the treatment doses of chiHEA125-Ama ranging from 10 to 100 μg/kg with respect to α-amanitin.

Because of high therapeutic efficacy and low toxicity, the site-specific delivery of anticancer agents to tumor cells is an emerging new therapeutic modality. In this study, we used chiHEA125 antibody directed against EpCAM because this transmembrane molecule is overexpressed in the majority of solid tumors. Several EpCAM-specific antibody-based molecular constructs have been developed and used for targeted delivery to tumor cells, for example, immunoliposomes (38), adenoviral vectors (39,40), enzymes (41), and cytokines (42). In addition, EpCAM-specific constructs have been used to deliver toxic proteins to tumors. One study describes a humanized anti-EpCAM Fab moiety linked to a de-immunized version of bouganin, VB6-845, with a potent antitumor efficacy (43). Patricia et al. (44) reported a potent antitumor activity of EpCAM-specific designed ankyrin repeat proteins (DARPins) (Ec4) as a fusion toxin with *P aeruginosa* exotoxin A (44). Intratumoral injection of scFv-Pseudomonas exotoxin A fusion construct VB4-845 to patients with squamous cell carcinoma of the head and neck showed positive response in 87.5% of patients in a phase I study (45). However, some patients developed neutralizing antibody to VB4-845. Therefore, small-molecule anticancer agents coupled to tumor-selective antibodies may have clinical advantage over immunoconstructs including large protein toxins. One example for such a small-molecule ADC is an anti-EpCAM antibody, conjugated with the maytansine analog DM1 to form an ADC, which after internalization and cleavage suppressed microtubule dynamics in MCF-7 breast tumor cells (46). α-amanitin, the toxin used in this study, is of comparable size as DM1 but varies in its target specificity. Different from many toxins

used in today's ADCs, which mainly act on the microtubule system, α-amanitin binds to and inhibits the eukaryotic RNA polymerase II. It is the most potent and specific inhibitor of the RNA polymerase II known so far. Therefore, since α-amanitin efficiently inhibits the transcription machinery in all mammalian cells at very low toxin concentrations, α-amanitin ADC would most likely act on both proliferating and quiescent tumor cells. Taken together, site-specific delivery of anti-cancer agents with EpCAM-specific constructs can evolve as a promising therapeutic strategy.

In chiHEA125-Ama, α-amanitin was attached to the immunoglobulin by an ester linkage intended to release free α-amanitin inside the tumor cell when in contact with esterases or proteases. An α-amanitin load (the number of amanitin molecules per IgG molecule) of up to eight molecules per chiHEA125 IgG molecule did not affect binding of chiHEA125-Ama to EpCAM-expressing tumor cells. Ratios higher than 8 were avoided because the affinity of such conjugates to tumor cells decreased. After binding to the cell surface, an internalization of the ADCs seems to occur based on the observations that ADCs were visualized in endosomal vesicles (47). Early experiments showed that amanitin conjugates of high molar mass are poor inhibitors of the transcription enzymes (48). Therefore, the high antiproliferative potency of chiHEA125-Ama found in our experiments suggests that proteolytic breakdown of the IgG carrier or hydrolysis of the ester linkage must occur in endosomal/lysosomal compartments. In contrast to protease-degradable protein toxins, α-amanitin remains unaffected by proteases. The cyclopeptide ring of the amatoxins withstands all common proteolytic enzymes (H. Faulstich, unpublished data). This stability against proteases, beside the low risk of immunogenicity, is certainly another great advantage of α-amanitin supporting its use as the drug component in ADCs.

At present, clinical application of many immunotoxins is hampered by their dose-limiting toxicity. Free α-amanitin causes apoptosis and necrosis of hepatocytes, which is one of the main reasons of fatality in human mushroom poisoning. Liver toxicity of free amatoxins is based on the presence of the transporting protein OATP1B3, which is expressed exclusively on the sinusoidal membrane of hepatocytes (49). In contrast, α-amanitin when coupled to proteins, including albumin, is no longer a substrate for OATP1B3, as shown in our laboratory using OATP1B3-transfected cell lines (J. Anderl, unpublished data). Instead, amanitin conjugates are preferentially taken up by protein-consuming cells such as macrophages and cells of the reticuloendothelial system (50,51). This effect may be envisaged as a potential cause of systemic toxicity of the α-amanitin-immunoglobulin conjugates. However, in vitro experiments with mouse macrophages showed that uptake of an albumin-β-amanitin conjugate will occur at concentrations of approximately 10^{-8} M (50), a concentration by orders of magnitude higher than the concentrations of chiHEA125-Ama as used in this study. Therefore, we aimed to minimize the α-amanitin-related toxicity by conjugating α-amanitin to an antibody that combined high specificity and high affinity for the tumor-associated antigen EpCAM. ChiHEA125-Ama succeeded to provide a high targeting effect for α-amanitin at concentrations probably too low to induce systemic toxicity. The absence of systemic side effects of chiHEA125-Ama treatment even at the high doses of 50 and 100 μg/kg, as well as the absence of critically elevated blood levels of liver enzymes, supports the potential of the concept presented in this study. Targeting of amanitin to specific cell types by conjugating the toxin to an IgG specific for the murine Thy 1.2 antigen was shown by Davis et al. (52), who achieved an enhancement of amanitin cytotoxicity by a factor of 500 over free amanitin but did not report on in vivo experiments. Interestingly, an amino derivative of phalloidin, a member of the second family of toxic cyclic peptides produced by *A phalloides* (28), when conjugated to chiHEA125, exhibited no cytotoxic effects to MCF-7 breast cancer cells up to concentrations of 10 μM (data not shown and J. Anderl, unpublished data).

We could rule out the possibility that the toxicity observed in mice treated with very high doses of chiHEA125-Ama (150 and 300 μg/kg) was caused by free α-amanitin, which could be eventually released from the ADC. This is based on the data that the total amount of conjugated α-amanitin administered to the mouse was below the LD50 value of α-amanitin (LD50 of free α-amanitin in nude mice is approximately 500 μg/kg after intraperitoneal injection) (29) (J. Anderl, unpublished data). Assuming that all conjugated α-amanitin was released from chiHEA125-Ama, such toxic LD50 concentrations would not be achieved. Furthermore, mammals excrete free amatoxins including α-amanitin (molecular weight = 919 Da, highly water soluble) very fast in urine. The half-life of α-amanitin in mice was determined to be about 30 minutes, rendering the accumulation of toxic concentrations unlikely. This should also apply to free α-amanitin potentially released from dying tumor cells after intracellular ADC breakdown.

One of the limitations of our study is that we cannot exclude that there will be a dose-limiting toxicity in human patients after the systemic administration of chiHEA125-Ama because of binding of ADC to EpCAM-positive epithelial cells in normal tissues, especially in pancreas, similar to that observed in clinical trials with unconjugated anti-EpCAM mAbs [reviewed in (15,16)]. However, locoregional delivery of VB4-845, an anti-EpCAM scFv-Pseudomonas exotoxin A fusion construct, was well tolerated in phase I studies by patients with nonmuscle-invasive bladder cancer (53) and by patients with squamous cell carcinoma of the head and neck after intratumoral VB4-845 injections (45). Furthermore, intraperitoneal injections of anti-EpCAMxCD3 bispecific antibody were well tolerated by advanced ovarian carcinoma patients (54). In addition, biodistribution studies of EpCAM-directed mAb in EpCAM-transgenic mouse B16 melanoma tumor model showed discrepancy in normal tissue distribution between two different humanized anti-EpCAM mAb MOC31-hFc and UBS54 (55). Nevertheless, experiments in an EpCAM-transgenic mouse tumor model of pancreatic carcinoma or in relevant species are needed to evaluate potential systemic toxicity of chiHEA125-Ama related to the targeting of EpCAM.

In conclusion, α-amanitin-conjugated chimerized anti-EpCAM mAb, chiHEA125-Ama, effectively eradicated experimental pancreatic carcinoma at low risk of systemic toxicity and could therefore become a novel anticancer agent for pancreatic cancer and for EpCAM-overexpressing carcinomas.

References

1. Jemal A, Siegel R, Xu J, Ward E. Cancer statistics, 2010. *CA Cancer J Clin.* 2010;60(5):277–300.
2. Michalski CW, Weitz J, Buchler MW. Surgery insight: surgical management of pancreatic cancer. *Nat Clin Pract Oncol.* 2007;4(9):526–535.

3. Trzpis M, McLaughlin PM, de Leij LM, Harmsen MC. Epithelial cell adhesion molecule: more than a carcinoma marker and adhesion molecule. *Am J Pathol.* 2007;171(2):386–395.
4. Baeuerle PA, Gires O. EpCAM (CD326) finding its role in cancer. *Br J Cancer.* 2007;96(3):417–423.
5. Balzar M, Winter MJ, de Boer CJ, Litvinov SV. The biology of the 17-1A antigen (Ep-CAM). *J Mol Med.* 1999;77(10):699–712.
6. Winter MJ, Nagtegaal ID, van Krieken JH, Litvinov SV. The epithelial cell adhesion molecule (Ep-CAM) as a morphoregulatory molecule is a tool in surgical pathology. *Am J Pathol.* 2003;163(6):2139–2148.
7. Went PT, Lugli A, Meier S, et al. Frequent EpCam protein expression in human carcinomas. *Human Pathol.* 2004;35(1):122–128.
8. Gastl G, Spizzo G, Obrist P, Dunser M, Mikuz G. Ep-CAM overexpression in breast cancer as a predictor of survival. *Lancet.* 2000;356(9246):1981–1982.
9. Varga M, Obrist P, Schneeberger S, et al. Overexpression of epithelial cell adhesion molecule antigen in gallbladder carcinoma is an independent marker for poor survival. *Clin Cancer Res.* 2004;10(9):3131–3136.
10. Spizzo G, Obrist P, Ensinger C, et al. Prognostic significance of Ep-CAM and Her-2/neu overexpression in invasive breast cancer. *Int J Cancer.* 2002;98(6):883–888.
11. Spizzo G, Went P, Dirnhofer S, et al. High Ep-CAM expression is associated with poor prognosis in node-positive breast cancer. *Breast Cancer Res Treat.* 2004;86(3):207–213.
12. Al-Hajj M, Wicha MS, Benito-Hernandez A, Morrison SJ, Clarke MF. Prospective identification of tumorigenic breast cancer cells. *Proc Natl Acad Sci U S A.* 2003;100(7):3983–3988.
13. Dalerba P, Dylla SJ, Park IK, et al. Phenotypic characterization of human colorectal cancer stem cells. *Proc Natl Acad Sci U S A.* 2007;104(24):10158–10163.
14. Li C, Heidt DG, Dalerba P, et al. Identification of pancreatic cancer stem cells. *Cancer Res.* 2007;67(3):1030–1037.
15. Armstrong A, Eck SL. EpCAM: a new therapeutic target for an old cancer antigen. *Cancer Biol Ther.* 2003;2(4):320–326.
16. Chaudry MA, Sales K, Ruf P, Lindhofer H, Winslet MC. EpCAM an immunotherapeutic target for gastrointestinal malignancy: current experience and future challenges. *Br J Cancer.* 2007;96(7):1013–1019.
17. Ammons WS, Bauer RJ, Horwitz AH, et al. In vitro and in vivo pharmacology and pharmacokinetics of a human engineered monoclonal antibody to epithelial cell adhesion molecule. *Neoplasia.* 2003;5(2):146–154.
18. Munz M, Murr A, Kvesic M, et al. Side-by-side analysis of five clinically tested anti-EpCAM monoclonal antibodies. *Cancer Cell Int.* 2010;10:44.
19. Oberneder R, Weckermann D, Ebner B, et al. A phase I study with adecatumumab, a human antibody directed against epithelial cell adhesion molecule, in hormone refractory prostate cancer patients. *Eur J Cancer.* 2006;42(15):2530–2538.
20. Marschner N, Ruttinger D, Zugmaier G, et al. Phase II study of the human anti-epithelial cell adhesion molecule antibody adecatumumab in prostate cancer patients with increasing serum levels of prostate-specific antigen after radical prostatectomy. *Urol Int.* 2010;85(4):386–395.
21. Schmidt M, Scheulen ME, Dittrich C, et al. An open-label, randomized phase II study of adecatumumab, a fully human anti-EpCAM antibody, as monotherapy in patients with metastatic breast cancer. *Ann Oncol.* 2010;21(2):275–282.
22. Shapira S, Shapira A, Starr A, et al. An immunoconjugate of anti-CD24 and Pseudomonas exotoxin selectively kills human colorectal tumors in mice. *Gastroenterology.* 2011;140(3):935–946.
23. Kovtun YV, Audette CA, Mayo MF, et al. Antibody-maytansinoid conjugates designed to bypass multidrug resistance. *Cancer Res.* 2010;70(6):2528–2537.
24. Francisco JA, Cerveny CG, Meyer DL, et al. cAC10-vcMMAE, an anti-CD30-monomethyl auristatin E conjugate with potent and selective antitumor activity. *Blood.* 2003;102(4):1458–1465.
25. Hamblett KJ, Senter PD, Chace DF, et al. Effects of drug loading on the antitumor activity of a monoclonal antibody drug conjugate. *Clin Cancer Res.* 2004;10(20):7063–7070.
26. Alley SC, Okeley NM, Senter PD. Antibody-drug conjugates: targeted drug delivery for cancer. *Curr Opin Chem Biol.* 2010;14(4):529–537.
27. Wieland T, Faulstich H. Amatoxins, phallotoxins, phallolysin, and antamanide: the biologically active components of poisonous Amanita mushrooms. *CRC Crit Rev Biochem.* 1978;5(3):185–260.
28. Wieland T. The toxic peptides from Amanita mushrooms. *Int J Pept Protein Res.* 1983;22(3):257–276.
29. Wieland T. *Peptides of Poisonous Amanita Mushrooms.* 1st ed. New York, NY: Springer-Verlag; 1986.
30. Walton JD, Hallen-Adams HE, Luo H. Ribosomal biosynthesis of the cyclic peptide toxins of Amanita mushrooms. *Biopolymers.* 2010;94(5):659–664.
31. Cochet-Meilhac M, Chambon P. Animal DNA-dependent RNA polymerases. 11. Mechanism of the inhibition of RNA polymerases B by amatoxins. *Biochim Biophys Acta.* 1974;353(2):160–184.
32. Cochet-Meilhac M, Nuret P, Courvalin JC, Chambon P. Animal DNA-dependent RNA polymerases. 12. Determination of the cellular number of RNA polymerase B molecules. *Biochim Biophys Acta.* 1974;353(2):185–192.
33. Magdalan J, Ostrowska A, Piotrowska A, et al. Alpha-amanitin induced apoptosis in primary cultured dog hepatocytes. *Folia Histochem Cytobiol.* 2010;48(1):58–62.
34. Moldenhauer G, Momburg F, Moller P, Schwartz R, Hammerling GJ. Epithelium-specific surface glycoprotein of Mr 34,000 is a widely distributed human carcinoma marker. *Br J Cancer.* 1987;56(6):714–721.
35. Momburg F, Moldenhauer G, Hammerling GJ, Moller P. Immunohistochemical study of the expression of a Mr 34,000 human epithelium-specific surface glycoprotein in normal and malignant tissues. *Cancer Res.* 1987;47(11):2883–2891.
36. Kirchner K, Faulstich H. Purification of amatoxin-specific antibodies from rabbit sera by affinity chromatography, their characterization and use in toxicological studies. *Toxicon.* 1986;24(3):273–283.
37. Salnikov AV, Groth A, Apel A, et al. Targeting of cancer stem cell marker EpCAM by bispecific antibody EpCAMxCD3 inhibits pancreatic carcinoma. *J Cell Mol Med.* 2009;13(9B):4023–4033.
38. Hussain S, Pluckthun A, Allen TM, Zangemeister-Wittke U. Antitumor activity of an epithelial cell adhesion molecule targeted nanovesicular drug delivery system. *Mol Cancer Ther.* 2007;6(11):3019–3027.
39. Haisma HJ, Pinedo HM, Rijswijk A, et al. Tumor-specific gene transfer via an adenoviral vector targeted to the pan-carcinoma antigen EpCAM. *Gene Ther.* 1999;6(8):1469–1474.
40. Heideman DA, Snijders PJ, Craanen ME, et al. Selective gene delivery toward gastric and esophageal adenocarcinoma cells via EpCAM-targeted adenoviral vectors. *Cancer Gene Ther.* 2001;8(5):342–351.
41. de Graaf M, Boven E, Oosterhoff D, et al. A fully human anti-Ep-CAM scFv-beta-glucuronidase fusion protein for selective chemotherapy with a glucuronide prodrug. *Br J Cancer.* 2002;86(5):811–818.
42. Schanzer JM, Fichtner I, Baeuerle PA, Kufer P. Antitumor activity of a dual cytokine/single-chain antibody fusion protein for simultaneous delivery of GM-CSF and IL-2 to Ep-CAM expressing tumor cells. *J Immunother.* 2006;29(5):477–488.
43. Cizeau J, Grenkow DM, Brown JG, Entwistle J, MacDonald GC. Engineering and biological characterization of VB6-845, an anti-EpCAM immunotoxin containing a T-cell epitope-depleted variant of the plant toxin bouganin. *J Immunother.* 2009;32(6):574–584.
44. Patricia MK, Stefan N, Rothschild S, Pluckthun A, Zangemeister-Wittke U. A novel fusion toxin derived from an EpCAM-specific designed ankyrin repeat protein has potent antitumor activity. *Clin Cancer Res.* 2011;17(1):100–110.
45. MacDonald GC, Rasamoelisolo M, Entwistle J, et al. A phase I clinical study of VB4-845: weekly intratumoral administration of an anti-EpCAM recombinant fusion protein in patients with squamous cell carcinoma of the head and neck. *Drug Des Devel Ther.* 2009;2:105–114.
46. Oroudjev E, Lopus M, Wilson L, et al. Maytansinoid-antibody conjugates induce mitotic arrest by suppressing microtubule dynamic instability. *Mol Cancer Ther.* 2010;9(10):2700–2713.
47. Austin CD, Wen X, Gazzard L, Nelson C, Scheller RH, Scales SJ. Oxidizing potential of endosomes and lysosomes limits intracellular cleavage of disulfide-based antibody-drug conjugates. *Proc Natl Acad Sci U S A.* 2005;102(50):17987–17992.
48. Faulstich H, Fiume L. Protein conjugates of fungal toxins. *Methods Enzymol.* 1985;112:225–237.

49. Letschert K, Faulstich H, Keller D, Keppler D. Molecular characterization and inhibition of amanitin uptake into human hepatocytes. *Toxicol Sci*. 2006;91(1):140–149.
50. Barbanti-Brodano G, Fiume L. Selective killing of macrophages by amanitin-albumin conjugates. *Nat New Biol*. 1973;243(130):281–283.
51. Barbanti-Brodano G, Derenzini M, Fiume L. Toxic action of a phalloidin-albumin conjugate on cells with a high protein uptake. *Nature*. 1974;248(443):63–65.
52. Davis MT, Preston JF III. A conjugate of alpha-amanitin and monoclonal immunoglobulin G to Thy 1.2 antigen is selectively toxic to T lymphoma cells. *Science*. 1981;213(4514):1385–1388.
53. Kowalski M, Entwistle J, Cizeau J, et al. A phase I study of an intravesically administered immunotoxin targeting EpCAM for the treatment of non-muscle-invasive bladder cancer in BCG-refractory and BCG-intolerant patients. *Drug Des Devel Ther*. 2010;4:313–320.
54. Marme A, Strauss G, Bastert G, Grischke EM, Moldenhauer G. Intraperitoneal bispecific antibody (HEA125xOKT3) therapy inhibits malignant ascites production in advanced ovarian carcinoma. *Int J Cancer*. 2002;101(2):183–189.
55. Kosterink JG, McLaughlin PM, Lub-de Hooge MN, et al. Biodistribution studies of epithelial cell adhesion molecule (EpCAM)-directed monoclonal antibodies in the EpCAM-transgenic mouse tumor model. *J Immunol*. 2007; 179(2):1362–1368.

Funding

This work was supported by the Initiative and Networking Fund of the Helmholtz Association within the Helmholtz Alliance on Immunotherapy of Cancer (LL_WP6b and LL_WP7b to GM).

Notes

G. Moldenhauer and A. V. Salnikov contributed equally to this work. We thank Elvira Hallauer, Sabine Ottinger, and Jury Gladkich for excellent technical assistance. The authors are solely responsible for the study design, data collection, analysis and interpretation of the data, writing the article, and decision to submit the article for publication.

J. Anderl is an employee of Heidelberg Pharma GmbH. H. Faulstich received licensing fees from Heidelberg Pharma GmbH. The other authors declare no conflict of interest.

Affiliations of authors: Department of Translational Immunology, German Cancer Research Center, Heidelberg, Germany (GM, AVS, SL); National Center for Tumor Diseases, Heidelberg, Germany (GM, AVS, SL); Molecular OncoSurgery Group, Department of General Surgery, University of Heidelberg and German Cancer Research Center, Heidelberg, Germany (AVS, IH); Heidelberg Pharma GmbH, Ladenburg, Germany (JA); Bioorganic Research Group, Max Planck Institute for Medical Research, Heidelberg, Germany (HF).